Improving the automatic inversion of digital Alouette/ISIS ionogram reflection traces into topside electron density profiles

Robert F. Benson,[1] Vladimir Truhlik,[2] Xueqin Huang,[3] Yongli Wang,[4] and Dieter Bilitza[5,6]

Received 6 December 2011; revised 8 February 2012; accepted 9 February 2012; published 30 March 2012.

[1] The topside sounders of the International Satellites for Ionospheric Studies (ISIS) program were designed as analog systems. The resulting ionograms were displayed on 35 mm film for analysis by visual inspection. Each of these satellites, launched between 1962 and 1971, produced data for 10 to 20 years. A number of the original telemetry tapes from this large data set have been converted directly into digital records. Software, known as the Topside Ionogram Scalar With True-Height (TOPIST) algorithm, has been produced and used for the automatic inversion of the ionogram reflection traces on more than 100,000 ISIS-2 digital topside ionograms into topside vertical electron density profiles $N_e(h)$. Here we present some topside ionospheric solar cycle variations deduced from the TOPIST database to illustrate the scientific benefit of improving and expanding the topside ionospheric $N_e(h)$ database. The profile improvements will be based on improvements in the TOPIST software motivated by direct comparisons between TOPIST profiles and profiles produced by manual scaling in the early days of the ISIS program. The database expansion will be based on new software designed to overcome limitations in the original digital topside ionogram database caused by difficulties encountered during the analog-to-digital conversion process in the detection of the ionogram frame sync pulse and/or the frequency markers. This improved and expanded TOPIST topside $N_e(h)$ database will greatly enhance investigations into both short- and long-term ionospheric changes, e.g., the observed topside ionospheric responses to magnetic storms, induced by interplanetary magnetic clouds, and solar cycle variations, respectively.

Citation: Benson, R. F., V. Truhlik, X. Huang, Y. Wang, and D. Bilitza (2012), Improving the automatic inversion of digital Alouette/ISIS ionogram reflection traces into topside electron density profiles, *Radio Sci.*, *47*, RS0L04, doi:10.1029/2011RS004963.

1. Introduction

[2] *Benson* [1996] and *Benson and Bilitza* [2009] describe a data restoration project that resulted in more than 1/2 million digital ionograms from the Alouette-2, ISIS-1, and ISIS-2 ionospheric topside sounders. These new digital records were produced from original seven-track analog telemetry tapes recorded between 1965 and 1984 from 24 globally distributed ground stations as part of the International Satellites for Ionospheric Studies (ISIS) program designed primarily to produce vertical topside electron density profiles $N_e(h)$ [*Jackson*, 1986, 1988; *Jackson and Warren*, 1969]. These digital data are available for viewing and downloading via links from the ISIS topside sounder data restoration project home page at http://nssdc.gsfc.nasa.gov/space/isis/isis-status.html.

[3] The purpose of this paper is to discuss the results from an inversion program, known as the Topside Ionogram Scaler With True-Height (TOPIST) algorithm, originally designed to process digital ISIS-2 ionograms [*Bilitza et al.*, 2004; *Huang et al.*, 2002]. TOPIST is a knowledge-based retrieval system that simulates the behavior of a human operator, rather than being based on neural network techniques. It is built on earlier experience with the analysis of topside ionograms and ionograms from ground-based Digisondes [*Huang and Reinisch*, 1982; *Reinisch and Huang*, 1982, 1983]. One of the challenges in the automatic scaling of the ISIS ionograms is to distinguish between the O and X mode traces since the data do not include wave polarization. The approach used by TOPIST is to first identify the plasma resonance frequencies and

[1]NASA Goddard Space Flight Center, Greenbelt, Maryland, USA.
[2]Institute of Atmospheric Physics, Academy of Sciences of the Czech Republic, Prague, Czech Republic.
[3]Center for Atmospheric Research, University of Massachusetts Lowell, Lowell, Massachusetts, USA.
[4]Goddard Planetary Heliophysics Institute, University of Maryland Baltimore County, NASA Goddard Space Flight Center, Greenbelt, Maryland, USA.
[5]School of Physics, Astronomy, and Computational Sciences, George Mason University, Fairfax, Virginia, USA.
[6]Also at NASA Goddard Space Flight Center, Greenbelt, Maryland, USA.

0048-6604/12/2011RS004963

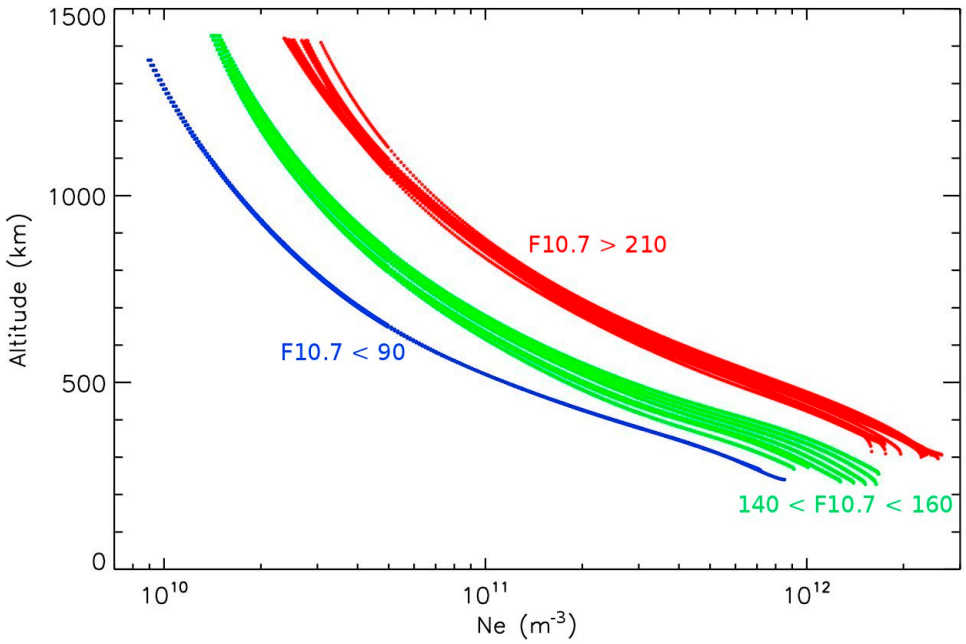

Figure 1. TOPIST topside $N_e(h)$ profiles corresponding to three different levels of solar activity as indicated by the 10.7 cm solar radio flux index (F10.7). The 2 blue, 7 green, and 14 red curves correspond to F10.7 ranges of <90, 140–160, and >210, respectively. The curves are based on TOPIST profiles of highest quality (quality flag = 3) automatically scaled from ISIS-2 digital ionograms recorded at low midlatitudes (magnetic latitude (MLAT) = 30 ± 5°), midday (magnetic local time (MLT) = 13 ± 1 h), during equinox intervals (equinox ± 5 days) contained in the interval from 18 February 1971 to 27 October 1984. (Two additional blue curves, corresponding to low solar activity, satisfying the data restriction conditions were excluded because of obvious problems encountered in the automatic identification of the proper wave cutoff conditions at the satellite.)

then use the general theory of radio wave propagation in a magnetoplasma to identify these traces. Once the two traces are identified, a leading edge algorithm determines the leading edges of the echo traces that are used as input for the profile inversion process, which uses both traces, to calculate $N_e(h)$ as described by *Bilitza et al.* [2004].

[4] In section 2 we present some TOPIST $N_e(h)$ profiles to illustrate the benefit of a large accurate database to detect solar cycle variations in the topside ionosphere, perform tests to check the accuracy of the TOPIST profiles, and illustrate improvements in the TOPIST software stimulated by these tests. In section 3 procedures are presented to correct problems encountered during the analog-to-digital (A/D) conversion process during the production of the digital ionogram files. A summary is presented in section 4.

2. The Value of TOPIST Profiles and Improving Their Accuracy

[5] As illustrated by *Benson and Bilitza* [2009, Figure 2a] there are more than 100,000 ISIS-2 TOPIST profiles available from 1971 to 1984, i.e., extending well past the peak of solar cycle 20 to well past the peak of cycle 21. These profiles are available from http://nssdc.gsfc.nasa.gov/space/isis/isis-status.html. The value of a large database of topside $N_e(h)$ profiles has been demonstrated using hand-scaled $N_e(h)$ profiles available from the NASA Space Physics Data Facility (SPDF) at the same address. These profiles are based on hand scaling, in the 1960s and 1970s, by skilled observers of more than 150,000 Alouette-1, Alouette-2, ISIS-1, and ISIS-2 topside ionograms as recorded on 35 mm film. A subset of the Alouette-2 $N_e(h)$ profiles from this database was used by *Bilitza et al.* [2004] to illustrate the need for improvements in the representation of the topside ionosphere in the International Reference Ionosphere (IRI). Such IRI improvements, based on all of the available $N_e(h)$ profiles from hand-scaled Alouette-1, Alouette-2, ISIS-1, and ISIS-2 topside ionograms, were made by *Bilitza* [2004, 2009] and *Bilitza et al.* [2006]. The large ISIS-2 TOPIST $N_e(h)$ profile database was used by *Reinisch et al.* [2007] to derive a topside model by matching the data to a Chapman function with continuously varying scale height. They combined this model with Radio Plasma Imager (RPI) measurements from the IMAGE satellite to construct a continuous topside N_e profile from several R_E altitude down to the F2 peak altitude.

[6] Figure 1 illustrates the benefit of a large TOPIST N_e topside profile database by showing the changes in low midlatitude, midday topside profiles for different levels of solar activity during equinox intervals over a solar cycle. The data used in Figure 1 were limited to only the highest-rated TOPIST profiles (see discussion below). The profiles within each solar activity level are seen to be remarkably consistent, even though they were collected over an interval of more than 13 years, when restricted to these narrow ranges of magnetic latitude, magnetic local time, and season. N_e is observed to increase at all altitudes, as would be expected, with increasing solar activity.

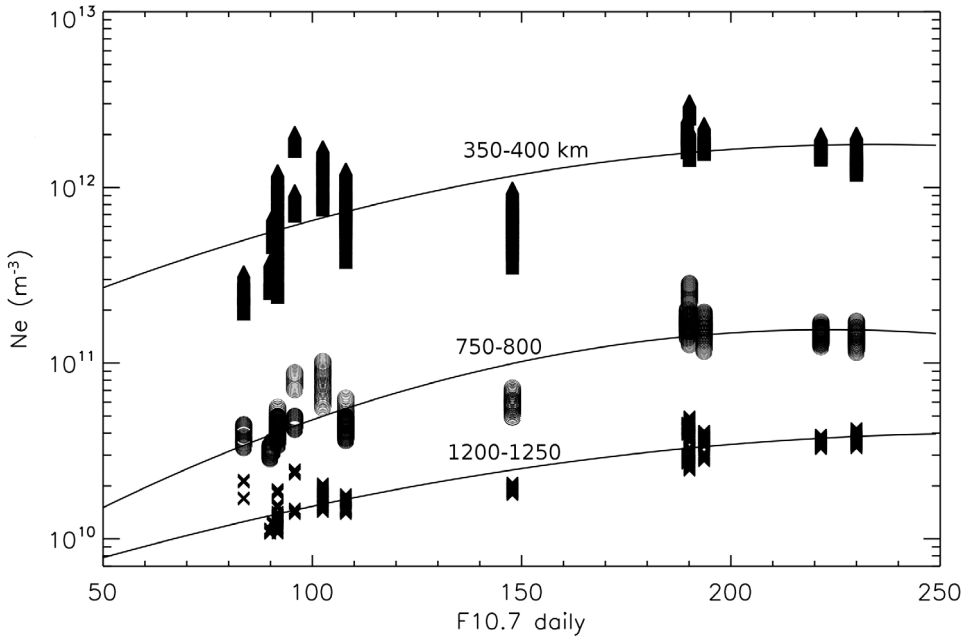

Figure 2. TOPIST topside N_e values in three different altitude ranges, 1200–1250, 750–800, and 350–400 km, for the crosses, circles, and triangles, respectively, versus the daily solar F10.7 index. The data are based on quality flag 3 TOPIST profiles corresponding to the same low midlatitude, midday, equinox intervals over the same long time interval (more than 13 years) as in Figure 1. The curves are fits to $\log N_e = a + b(F10.7) + c(F10.7)^2$ with a, b, and c values of 10.928, 1.123×10^{-2}, and -2.396×10^{-5}, respectively, for the low-altitude range; 9.511, 1.503×10^{-2}, and -3.362×10^{-5}, respectively, for the midaltitude range; and 9.523, 8.175×10^{-3}, and -1.551×10^{-5}, respectively, for the high-altitude range.

[7] In Figure 2 the above solar cycle variation is presented in a different way. The same low midlatitude, midday, equinox intervals were used as in Figure 1. In Figure 2, however, only N_e values from 50 km intervals corresponding to lower, middle, and upper portions of the profiles are presented versus the changing level of solar activity over a solar cycle. It is seen that for these low midlatitude, midday, equinox conditions that the increasing N_e with increasing F10.7 in the 350–400 and 750–800 km altitude ranges saturates around an F10.7 value of 220 but a similar saturation is not observed in the higher-altitude range of 1200–1250 km (the lowest curve in Figure 2).

[8] The success of such endeavors depends on the accuracy of the N_e profiles and on the size of the database. The accuracy of the TOPIST profiles was checked by comparing them to hand-scaled $N_e(h)$ profiles available from the NASA SPDF. Unfortunately, only several hundred cases were available for such comparisons. The reason for this limitation was that the selection of ISIS-2 telemetry tapes for A/D conversion into digital ionograms emphasized time intervals where few hand-scaled $N_e(h)$ profiles were available (in order to maximize the number of available topside $N_e(h)$ profiles) [Benson, 1996]. Thus only a few tenths of a percent of the available hand-scaled and TOPIST-derived $N_e(h)$ profiles were produced from the same ionogram data and could be directly compared; the former being based on ionogram data displayed on 35 mm films and the latter being based on digital files obtained from the same original seven-track analog telemetry tapes used decades ago to generate the 35 mm films.

[9] Our comparisons between the hand-scaled and the TOPIST-scaled ionograms were based mainly on the N_e values at the top of the profiles; that is, we compared the N_e values at the satellite altitude $(N_e)_{sat}$ because of their importance in obtaining a good topside $N_e(h)$ profile from a satellite-borne ionospheric topside sounder [see, e.g., *Jackson*, 1969]. These values can be determined very accurately from the plasma resonances and wave cutoffs observed on the ionograms as illustrated for an ISIS-2 ionogram by *Benson and Osherovich* [2004]. The main resonances are observed at the electron cyclotron frequency f_H, the electron plasma frequency f_N, and the upper hybrid frequency f_T where

$$f_T^2 = f_N^2 + f_H^2. \tag{1}$$

[10] The cutoff frequencies f_Z and f_X of the two branches of the extraordinary mode (X) can be used to determine f_N from the expressions

$$f_N^2 = f_X(f_X - f_H) \tag{2}$$

$$f_N^2 = f_Z(f_Z + f_H) \tag{3}$$

which can be combined to yield

$$f_H = f_X - f_Z. \tag{4}$$

Table 1. Selected Hand-Scaled (HS) and TOPIST-Scaled Topside Ionogram Quality Flags, Number of Comparisons Available, and Number of Profiles With Top-of-Profile N_e Differences Less Than 10%, Less Than 20%, or Greater Than a Factor of 2[a]

Quality Flags			Percentage of $N_e(h)$ Profiles With $\Delta(N_e)_{sat}$		
HS	TOPIST	Number of Comparisons	<10%	<20%	>Factor 2
All	all	248	22%	43%	>34%
All	3	60	>51%	76%	>13%
4 or 5	3	42	55%	>85%	<2.5%

[a]Top-of-profile N_e percent difference, i.e., at the satellite altitude, were calculated from $D(N_e)_{sat}$ = {(TOPIST − hand scaled)/(hand scaled)} × 100.

[11] Assuming that the gradients in f_N and f_H due to the satellite motion between the times when the above features are measured can be neglected, which is not always the case [e.g., see *Benson*, 1985, Figure 3b], an accurate (within about 2%) value of f_N can be determined which leads to an accurate value of $(N_e)_{sat}$ from

$$(N_e)_{sat}(m^{-3}) \approx (10^{12}/80.6) f_N(\mathrm{MHz})^2. \quad (5)$$

[12] Since the above relations provide 4 independent ways of determining f_N, and hence $(N_e)_{sat}$, from (5), i.e., from the observed f_N resonance, from the observed f_T resonance and (1), and from the observed X and Z wave cutoffs and (2) and (3), $(N_e)_{sat}$ can usually be determined with great confidence. This $(N_e)_{sat}$ determination, which can be made to an accuracy of about 4%, was used as the reference value by *Donley et al.* [1969] in their comparison of in situ techniques for determining N_e in space.

[13] When making comparisons between the TOPIST and hand-scaled topside $N_e(h)$ profiles, it is best to use the highest-quality ionogram data that were used to produce the profiles. Different rating schemes were used for the hand-scaled and TOPIST $N_e(h)$ profiles which can lead to confusion because higher numbers for the quality flags in the former indicate lower confidence in the $N_e(h)$ profiles whereas in the latter case they indicate higher confidence. The quality flag for the hand-scaled profiles ranged "from 4 for the best quality to 9 for those ionograms which provide minimal information concerning the electron density information" mainly due to "spread F and other phenomena which complicate the ionograms"; ionograms with quality flags from "7 to 9 should be used with caution" (Communications Research Centre, Ottawa, unpublished report, 1960s). The quality flag for the TOPIST $N_e(h)$ profiles ranged from 1 to 3 with 3 representing the highest confidence. The TOPIST flags are defined as follows: flag = 1 indicates the O and/or X traces have severe spread F (averaging more than twenty 3.75 km range bins per frequency) or the recalculated traces based on the inverted $N_e(h)$ profile deviate from the automatically scaled traces by a large amount (averaging more than 20 range bins per frequency); flag = 2 indicates that the above conditions are not satisfied but either the TOPIST-derived F2 peak differs from the modeled value by more than 50 km or the real foF2 value is most likely beyond the maximum swept frequency based on the scaled trace cusp shape; and flag = 3 if none of the above are true. The values in Table 1 indicate that even though the number of possible direct comparisons decreases when only high-quality profiles are considered, very good results are obtained, namely, 55% of the N_e values at the satellite altitude agreed within 10%, and more than 85% agreed within 20%, while only one example (representing 2.5%) differed by more than a factor of 2. Three comparisons were examined in detail: one where the differences were less than 5% and two where large differences were observed. All of these ionograms were in the extended sweep mode, i.e., from 0.1 to 20 MHz, and the ionogram frame sync pulses and all of the 22 frequency markers were properly identified during the A/D conversion process.

[14] In addition to comparing the TOPIST and hand-scaled $N_e(h)$ profiles a digital ionogram analysis program, available from the ISIS data restoration home page, was used to independently determine $(N_e)_{sat}$ from sounder-stimulated plasma resonances and wave cutoff frequencies using (1)–(5). The first example, where the TOPIST and the hand-scaled $N_e(h)$ profiles agree within 5% at the satellite position is presented in Figure 3. In addition to comparing N_e at the satellite altitude, the average % differences between the hand-scaled and the automatic TOPIST-scaled profiles was determined by calculating the absolute values of the percent differences between the two profiles (relative to the hand-scaled values) for each point on the profile. This average difference between the profiles was also found to agree within 5% for the case presented in Figure 3. Also presented in Figure 3 is the resonance-determined N_e at the satellite altitude; it is in good agreement with the N_e values for both profiles at this altitude.

[15] The next two examples, where large differences were observed between the TOPIST- and hand-scaled $N_e(h)$ profiles, are presented in Figures 4 and 5.

[16] The TOPIST profile of Figure 4 was in error because f_T was identified as f_N (the correct f_N resonance was not identified because it merged with f_H) and a clear O trace leading right up to f_N (a fairly rare occurrence) was apparently identified as a Z trace.

[17] The TOPIST profile of Figure 5 was in error because the strong diffuse resonance often observed between f_N and f_T when f_N/f_H is between about 0.7 and 1.3, and known as the DNT resonance [*Benson*, 1982], was identified as f_T. The f_X at the satellite was then taken as merging with the strong f_T resonance. The DNT resonance is not labeled in Figure 5 but is observed as a diffuse signal (strongest on the scan lines with frequencies 0.927 and 0.935 MHz) on the low-frequency side of the f_T resonance labeled "T" and slightly above the Z infinity wrap-around signal (also not labeled in Figure 5) that appears as a strong long-duration narrowband resonance (at 0.862 MHz) on the high-frequency side of the strong combined signal due to the f_H and f_N resonances

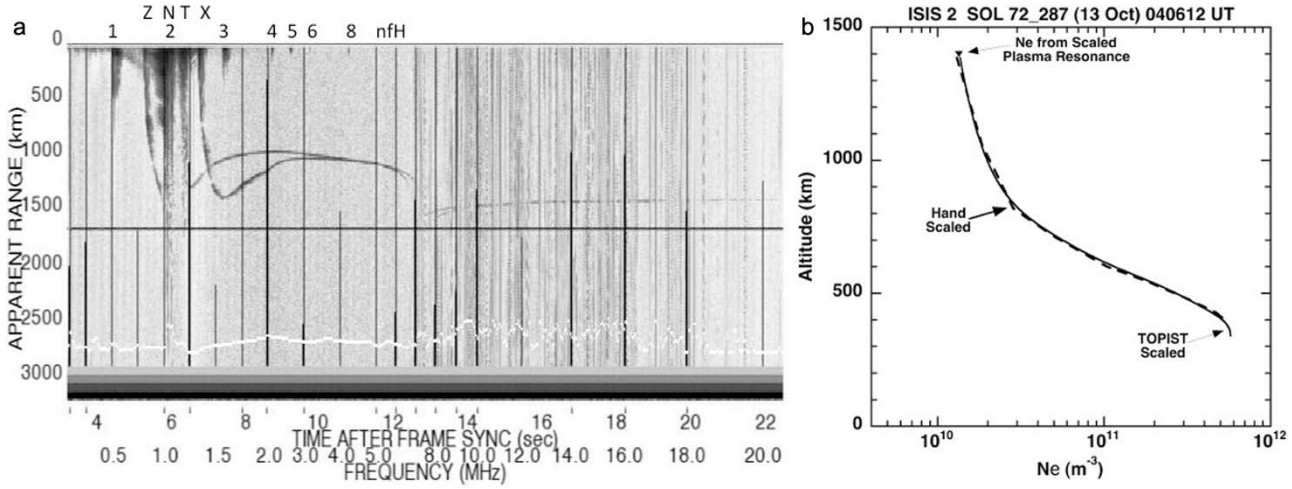

Figure 3. (a) ISIS-2 digital ionogram with resonance-determined values for $f_N/f_H = 1.039/0.524 = 1.98$ (the model value for $f_H = 0.521$ MHz). The symbols Z, N, T, and X at the top of the ionogram designate the cutoff and resonant frequencies f_Z, f_N, f_T, and f_X, respectively, used in equations (1)–(5); the numbers below these symbols designate the harmonics of f_H used in equations (1)–(4). The wavy white trace near the bottom of the ionogram corresponds to the sounder-receiver automatic gain control (AGC) voltage. (b) $N_e(h)$ profiles based on TOPIST automatic scaling and manual scaling by trained operators from the 1960s and 1970s (labeled hand scaled) and N_e at the satellite position based on inspection of resonances and cutoff frequencies. The latter indicated $f_N = 1.039$ MHz or, from (5), $N_e = 1.339 \times 10^{10}$ m^{-3}; the corresponding TOPIST values were $f_N = 1.047$ MHz and $N_e = 1.360 \times 10^{10}$ m^{-3} (SOL, 1972, day 287, 0406:12 UT).

labeled "1" and "N," respectively. The Z-infinity signal is called "wrap around" because it appears even at low apparent ranges due to an extension of the time base from the previous pulse [*Jackson*, 1969].

[18] Thus the large differences observed between the TOPIST and hand-scaled profiles in Figures 4 and 5 were due to the misidentification of the plasma resonances and wave cutoffs dependent on f_N when f_N/f_H was close to unity.

[19] In the version of TOPIST used for Figures 3–5 the time durations of plasma resonances and other features were determined, for each frequency scan line, by locating the greatest range bin below which no five consecutive bins with zero amplitude were found. (Note that after applying an efficient noise-filtering subroutine within TOPIST the ionogram is, in general, very clear because most of the range bin amplitudes are zero except where plasma resonances or echo traces are encountered.) The model f_H value and another resonance or wave cutoff, e.g., f_N or f_X, were then used as the two independent variables to create a comb filter with, typically, five frequency elements satisfying equations (1)–(3). The comb filter, for example, could consist of the elements f_Z, f_H, f_N, f_T, and $2f_H$. Starting with the model f_H

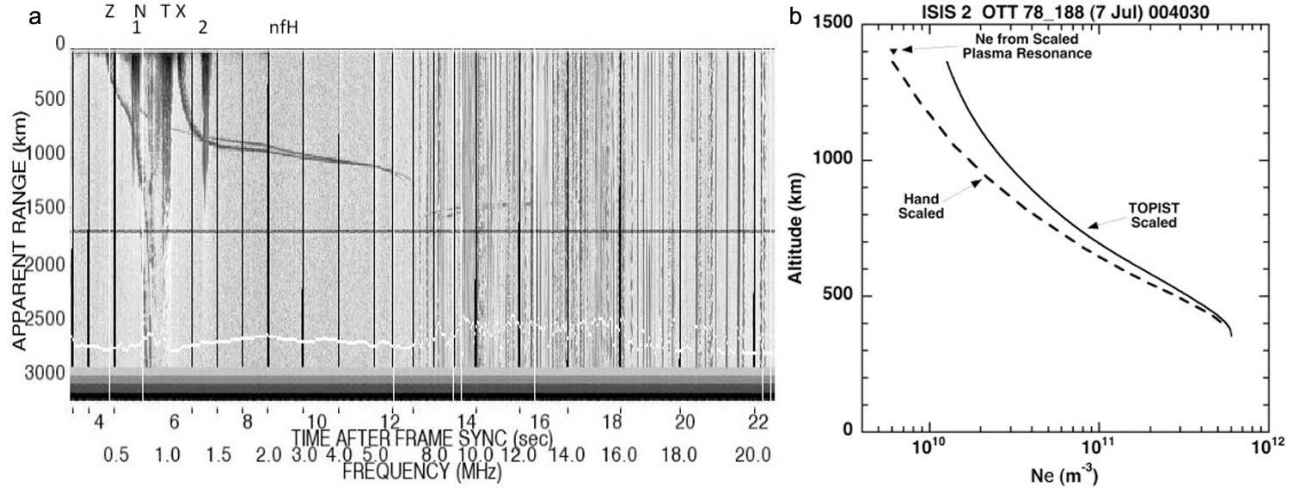

Figure 4. Same as Figure 3 except (a) $f_N/f_H = 0.702/0.685 = 1.02$ and $(f_H)_{model} = 0.663$ MHz). (b) $f_N = 0.702$ MHz corresponds to $N_e = 6.114 \times 10^9$ m^{-3}; the corresponding TOPIST values were $f_N = 1.008$ MHz and $N_e = 1.261 \times 10^{10}$ m^{-3} (OTT, 1978, day 188, 0040:30 UT).

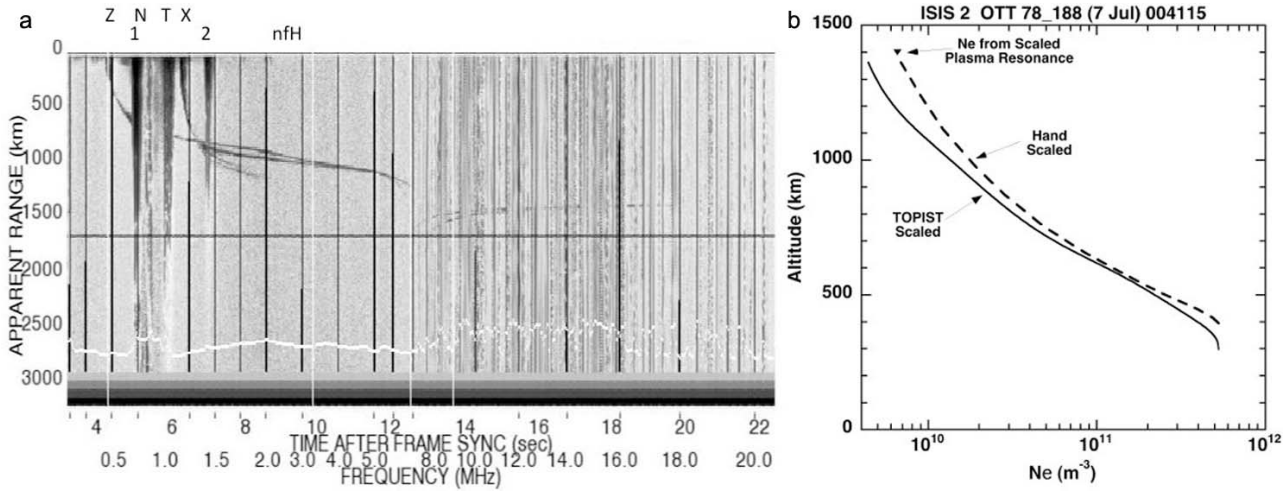

Figure 5. Same as Figure 4 except (a) f_N/f_H = 0.726/0.715 = 1.02 and $(f_H)_{model}$ = 0.685 MHz). (b) f_N = 0.726 MHz corresponds to $N_e = 6.539 \times 10^9$ m^{-3}; the corresponding TOPIST values were f_N = 0.594 MHz and $N_e = 4.378 \times 10^9$ m^{-3} (OTT, 1978, day 188, 0041:15 UT).

value, another resonant or cutoff value was then varied over allowed values, and the frequency positions of all the elements of the comb filter varied according to equations (1)–(3). A possible scenario would be to use f_T as the second independent variable and let it vary from its minimum value near f_H to a reasonable upper limit (taken as 2 MHz for ISIS 2). Each element of the comb filter had a bandwidth of five frequency scan lines consisting of two frequency scan lines on each side of the center frequency. A summation was then made of the signal amplitudes in all of the range bins, out to the greatest range bin determined earlier, for each of the five frequency scan lines for each of the elements of the comb filter for each position of the comb filter. Thus, if the comb filter consisted of five elements, each summation would be formed by summing amplitudes from 25 frequency scan lines; the exception being if two resonant or cutoff features were separated by less than five scan lines, then the amplitudes in the overlapping frequency scan lines were only counted once. The comb filter position producing the largest amplitude summation was considered as providing the best solution for determining the correct frequencies for the plasma resonances and wave cutoffs. Included in this procedure was a slight variation of the model f_H value because it often deviates from the actual value as determined from the observed nf_H sounder-stimulated plasma resonances. It was found, however, that in some cases the summation maximum did not correspond to the correct set of resonance and cutoff frequencies. These incorrect starting conditions cause scaling errors in the automatic identification of the ionospheric reflection traces and produce erroneous topside $N_e(h)$ profiles.

[20] In order to overcome this problem the TOPIST resonance detection algorithm was modified. The first modification was in the routine used for determining the maximum time duration of the plasma resonances. A sliding window, consisting of five consecutive apparent range bins, is slid along the ionogram apparent range axis in the direction of increasing apparent range. As the received signal amplitude in a plasma resonance decreases with distance, the maximum of the amplitude summation within the sliding apparent range window will occur at a smaller apparent range than the maximum apparent range for that resonance. If the signal amplitude summation in the window falls to less than half of the maximum value found on that particular frequency scan line, then that window position is identified as the plasma resonance maximum time duration. The second modification was to determine five sets of resonance and cutoff locations based on the five largest amplitude summations found by the above-described comb filter operation. It is likely that the correct set of resonance and cutoff frequencies corresponds to one of them. In order to determine which one gives the real resonance lines, each of these five possible sets was used to determine the starting values for the O and X traces and to automatically scale both of these traces. These traces were then inverted to produce $N_e(h)$ profiles and the profiles were used to recalculate the traces. The echo amplitudes contained in the first half of the recalculated traces (with 5 range bin width) were then summed for each of the five sets of possible resonance and cutoff locations. The largest echo amplitude summation was selected as the desired result. The resulting TOPIST profiles for the comparisons of Figures 4 and 5 are greatly improved while the good results of Figure 3 are slightly degraded but still very acceptable as illustrated in Figure 6 and Table 2.

[21] The first row of Table 2 indicates that the difference at the satellite altitude for the good example of Figure 3 becomes larger for TOPIST2 than for TOPIST. The larger difference, however, is still acceptable and is the smallest of all 3 comparisons. The differences for the other two comparisons (second and third rows in Table 2) are greatly reduced using TOPIST2. Additional improvements to the plasma resonance detection portion of TOPIST are planned, e.g., by increasing the options of resonances to use in the comb filter, in order to improve the crucial starting point for the inversion of ionospheric reflection traces to $N_e(h)$ profiles.

3. Correcting Problems Encountered During the Topside Ionogram A/D Conversion Process

[22] TOPIST was designed to process the swept frequency portion of ISIS-2 digital ionograms. Unfortunately,

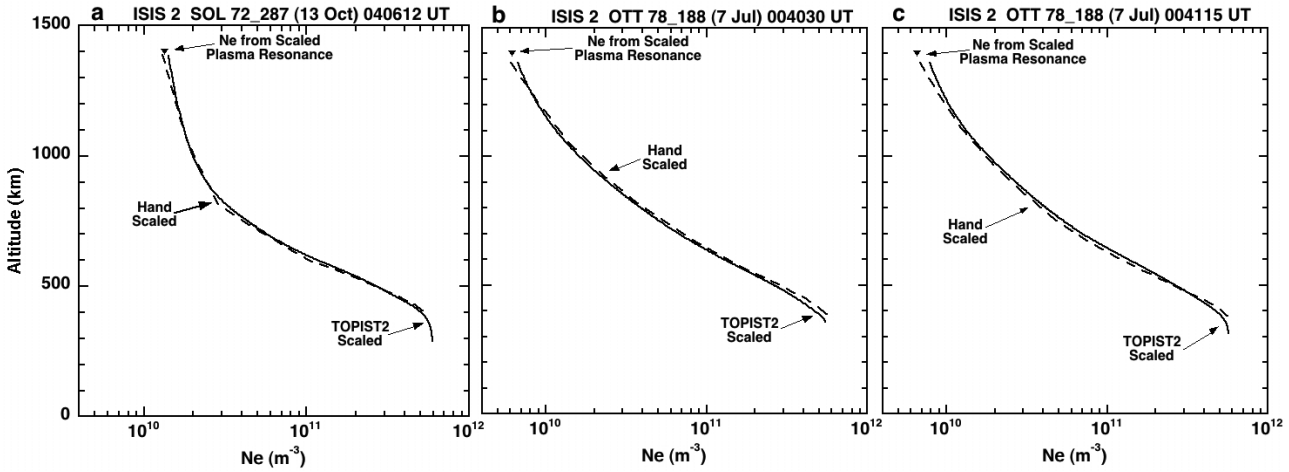

Figure 6. N_e(h) profiles based on revised TOPIST (labeled TOPIST2) and manual scaling and N_e at the satellite position based on plasma resonances. (a) Revision of Figure 3b, (b) revision of Figure 4b, and (c) revision of Figure 5b.

problems were often encountered in the identification of the frequency markers (superimposed on the receiver video output) during the A/D operation. A proper identification was required, however, because interpolation was performed between these markers to obtain the frequency of the intervening sounder-receiver amplitude scan lines.

[23] Two problems caused most of the TOPIST failures: (1) more than the expected number of frequency markers were detected and (2) the ionogram frame sync pulse (indicating the start of an ionogram) was not detected. In either case no frequency interpolation was performed (the scan line frequencies were set to a default value) and thus could not be processed by TOPIST. Figures 7 and 8 illustrate these two cases using ionograms from ISIS1 (the situations depicted apply to ISIS 2 as well). Figure 7 shows an ionogram that could not be processed because no frequency interpolation between markers was performed during the original A/D operation due to the extraneous frequency marker caused by a noise spike between the 8.0 and 9.0 MHz frequency markers.

[24] Figure 8 illustrates a problem caused by the lack of ionogram frame sync detection. In this example the file starts at 1.0 MHz on one ionogram and ends between the 1.75 and 2.0 MHz frequency markers on the following ionogram.

[25] Based on the experience gained with the ISIS-2 data, particularly the problems of the type illustrated by Figure 7, the frequency interpolation procedure was modified for ISIS 1. The frequency markers, and the times associated with them, are identified in the sounder video for both ISIS 1 and ISIS 2. A comparison is then made between their times and the times from a preestablished frequency marker table. This table contains times based on the hand scaling of the exact frequency marker onset times as seen on receiver amplitude scan lines containing frequency markers of a representative ionogram. In the case of ISIS 2, direct comparisons were made between the detected times and the times from the table. This comparison was not made, however, if more frequency markers were detected than were expected (as in the example of Figure 7) and, in the case of ISIS 2, no frequency interpolation was performed and TOPIST could not process the record.

[26] The comparison in the case of ISIS 1 consisted of calculating the time differences between adjacent identified frequency markers (the delta times) and comparing them to the delta times of the hand-scaled frequency markers from the reference table. This is a one-to-one comparison starting with the delta time between the 2nd and 1st identified frequency markers (0.25 and 0.1 MHz, respectively) and continuing through the rest of the delta times. If the delta time comparison failed, no further comparison was performed and the identified frequency markers prior to the failure were considered "good" and were used for the frequency interpolation for the intervening scan lines.

[27] Thus the digital ionogram in Figure 7, since it is from ISIS 1, will contain good frequency values up to 8.0 MHz and then default values for higher frequencies. Since the ionospheric echoes occur in the region below 8 MHz (there are some weaker ground returns at higher frequencies), TOPIST has been modified to process such ISIS-1 ionograms. If the same condition occurred in ISIS 2, as is often the case, no frequency interpolation was performed and TOPIST cannot process the ionogram.

[28] Software has been written to modify such ISIS-2 files, so they can be processed by TOPIST, by (1) using the identified frequency marker times included in the ISIS-2 files to calculate the delta times and perform the check described above to determine the good frequency markers, (2) perform frequency interpolations between these frequency markers

Table 2. Comparison of the Percent Differences in N_e at the Satellite Based on the Original Version of TOPIST and the Revised Version (TOPIST2)

Comparison Figures	TOPIST (% Difference)	TOPIST2 (% Difference)
Figures 3b and 6a	4.7	8.8
Figures 4b and 6b	109.2	10.4
Figures 5b and 6c	−36.1	14.7

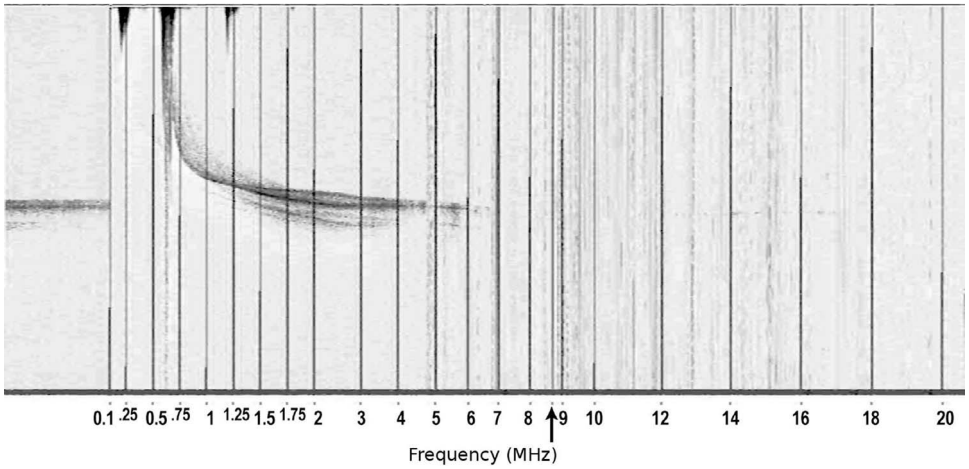

Figure 7. ISIS-1 digital ionogram with false frequency marker (arrow) between 8.0 and 9.0 MHz. The tick marks indicate features identified as frequency markers in the A/D process. (Ottawa, 21 January 1970, 1637:09 UT, 61.2° latitude, −115.1° longitude, 2590 km altitude.)

and create new files containing the proper frequency values up to the last good frequency, and (3) process the portion of the ionogram containing good frequencies using an ISIS-1 type version of TOPIST.

[29] Based on our ISIS-1 experience, the above modification will result in a major increase in the number of ISIS-2 ionograms that will be able to be processed since extraneous frequency markers mainly occur in the frequency domain above the ionospheric penetration frequency.

[30] Previously, the problem represented by Figure 8 could only be fixed manually by identifying the frame sync pulses separating the ionograms and creating files that could be spliced together. It was then necessary to identify the frequency markers and create an ionogram file with proper frequency interpolation as described above. While this operation was straight forward for an experienced observer, it was a time-consuming process. Software has now been written to perform this operation automatically. The results of applying this software to several ISIS-1 files, including the one in Figure 8, are presented in Figure 9.

[31] In Figure 9, the first portion of Figure 9b was digitally spliced to data from the previous file to produce the complete ionogram in Figure 9a and the last portion was spliced to data from the following file to produce the complete ionogram in Figure 9c. The times of the frequency markers in the resulting complete ionograms were then used to perform frequency interpolations for each topside sounder delay time scan line in order to produce ionograms with correct frequency information suitable for automatic processing by TOPIST. The software used to make the file corrections indicated in Figure 9 now makes it feasible to process more than 1/2 million Alouette-2, ISIS-1, and ISIS-2 digital topside ionogram files to check, and correct if necessary, the frequency information. Since the digital file repair process is just starting, statistical results based on corrections of the type illustrated in Figure 9 are not available. Once completed, however, the combination of TOPIST software improvements and a large TOPIST-friendly digital ionogram database will yield a TOPIST $N_e(h)$ profile database that will enable a wide range of long-term statistical studies of the

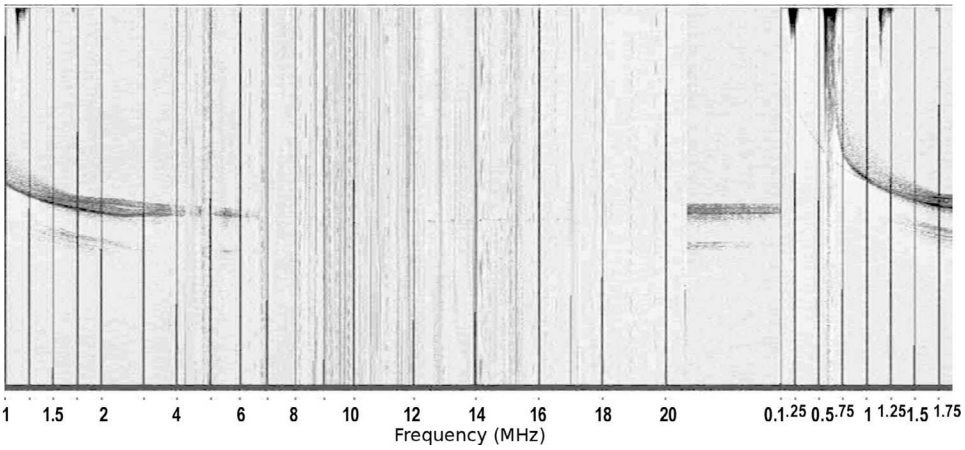

Figure 8. Partial ISIS-1 digital ionograms due to lack of frame sync identification. (Ottawa, 21 January 1970, 1635:24 UT, 0747 MLT, 57.0° latitude, −115.1° longitude, 2698 km altitude.)

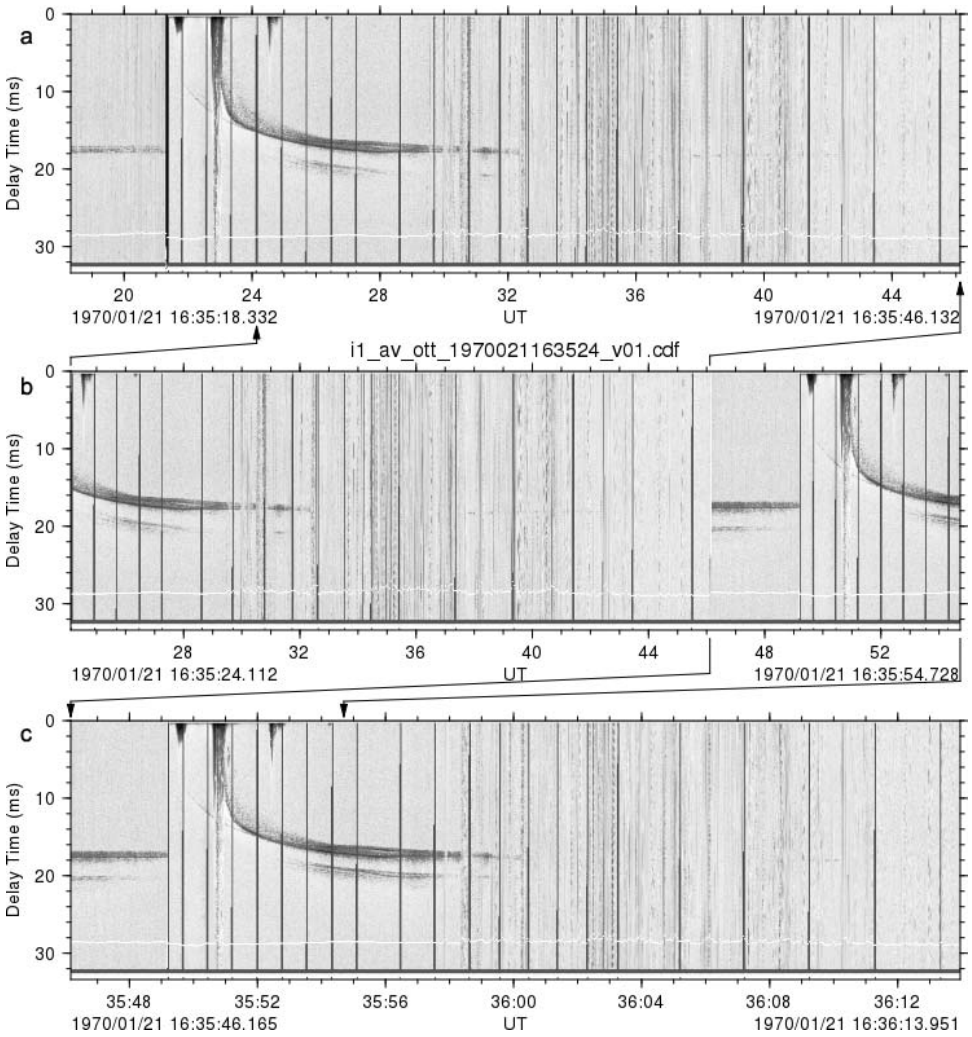

Figure 9. (a and c) Two correct ISIS-1 ionogram files created from (b) the partial ionograms of Figure 8 and earlier and later files as indicated by the arrows. Start and stop times for each of the above files are indicated at the bottom left and bottom right of each file, respectively.

type illustrated in Figures 1 and 2 as well as correlation studies involving multiple data sets [see, e.g., *Benson et al.*, 2011].

4. Conclusions

[32] More than 100,000 topside ionospheric $N_e(h)$ profiles available from the NASA SPDF Web site at http://nssdc.gsfc.nasa.gov/space/isis/isis-status.html, based on earlier automatic scaling of digital ISIS-2 topside ionograms using the TOPIST software, have been used to demonstrate the use of this database for investigating the ionospheric response to solar cycle variations. Low midlatitude, midday topside $N_e(h)$ profiles collected during a few days around each equinox interval over an interval of more than 13 years were remarkably consistent when restricted to narrow ranges of solar activity as reflected in the F10.7 index. The increasing N_e with increasing F10.7 in the lower altitude ranges saturates around an F10.7 value of 220 but a similar saturation was not observed in a higher-altitude sample (1200–1250 km). The tiny overlap between the above TOPIST database and the equally large database of topside $N_e(h)$ profiles available from the same Website, based on earlier manual scaling of 35-mm film ISIS-2 topside ionograms, were used to investigate the quality of the automatic TOPIST inversion of the ionospheric reflection traces into $N_e(h)$ profiles. When only $N_e(h)$ profiles with the highest-quality flags were considered, the N_e values at the satellite altitude (typically 1400 km) obtained from the hand-scaled and the TOPIST-scaled ionograms agreed within 20% on more than 85% of the available 42 comparisons. An investigation of the few comparisons with large discrepancies identified problems in the plasma resonance and wave cutoff determination procedure used by TOPIST. This procedure was then improved, leading to much better TOPIST results. A large problem encountered in the production of TOPIST topside $N_e(h)$ profiles, at no fault of TOPIST, is that many of the topside Alouette 2, ISIS-1, and ISIS-2 digital ionogram files do not contain proper frequency information as a result of problems encountered during the A/D conversion during the creation of the digital files. Two main causes of this lack of frequency information were illustrated as well as the results of software

that has been developed to remedy the situation. The plan is to apply this digital file correction software to the Alouette/ISIS digital topside ionogram database, and then use the improved TOPIST software to provide a large reliable topside ionospheric $N_e(h)$ profile database. Augmenting the existing hand-scaled data with this new TOPIST database should yield more than 1/2 million topside ionospheric $N_e(h)$ profiles spanning an interval of two solar cycles.

[33] **Acknowledgments.** This work was supported by the NASA Heliospheric Geospace Science Research Program. V.T. was supported, in part, by grant P209/10/2086 of the Grant Agency of the Czech Republic. The Interactive Data Language (IDL) program for Alouette/ISIS digital ionogram analysis, used in this work by R.F.B., was written by Gary Burgess at the GSFC.

References

Benson, R. F. (1982), Stimulated plasma instability and nonlinear phenomena in the ionosphere, *Radio Sci.*, *17*, 1637–1659, doi:10.1029/RS017i006p01637.

Benson, R. F. (1985), Field-aligned electron density irregularities near 500 km: Equator to polar cap topside sounder Z mode observations, *Radio Sci.*, *20*, 477–485, doi:10.1029/RS020i003p00477.

Benson, R. F. (1996), Ionospheric investigations using digital Alouette/ISIS topside ionograms, in *1996 Ionospheric Effects Symposium*, edited by J. M. Goodman, pp. 202–209, Technol. for Commun. Int., Alexandria, Va.

Benson, R. F., and D. Bilitza (2009), New satellite mission with old data: Rescuing a unique data set, *Radio Sci.*, *44*, RS0A04, doi:10.1029/2008RS004036.

Benson, R. F., and V. A. Osherovich (2004), Application of ionospheric topside-sounding results to magnetospheric physics and astrophysics, *Radio Sci.*, *39*, RS1S28, doi:10.1029/2002RS002834.

Benson, R. F., J. Fainberg, V. A. Osherovich, V. Truhlik, Y. Wang, D. Bilitza, and R. T. Arbacher (2011), Changes in the high-latitude topside ionospheric electron-density profiles in response to solar-wind perturbations during large magnetic storms, Abstract SM33B-06 presented at 2011 Fall Meeting, AGU, San Francisco, Calif., 5–9 Dec.

Bilitza, D. (2004), A correction for the IRI topside electron density model based on Alouette/ISIS topside sounder data, *Adv. Space Res.*, *33*, 838–843, doi:10.1016/j.asr.2003.07.009.

Bilitza, D. (2009), Evaluation of the IRI-2007 model options for the topside electron density, *Adv. Space Res.*, *44*, 701–706, doi:10.1016/j.asr.2009.04.036.

Bilitza, D., X. Huang, B. W. Reinisch, R. F. Benson, H. K. Hills, and W. B. Schar (2004), Topside ionogram scaler with true height algorithm (TOPIST): Automated processing of ISIS topside ionograms, *Radio Sci.*, *39*, RS1S27, doi:10.1029/2002RS002840.

Bilitza, D., B. W. Reinisch, S. M. Radicella, S. Pulinets, T. Gulyaeva, and L. Triskova (2006), Improvements of the International Reference Ionosphere model for the topside electron density profile, *Radio Sci.*, *41*, RS5S15, doi:10.1029/2005RS003370.

Donley, J. L., L. H. Brace, J. A. Findlay, J. H. Hoffman, and G. L. Wrenn (1969), Comparison of results of Explorer XXXI direct measurement probes, *Proc. IEEE*, *57*, 1078–1084, doi:10.1109/PROC.1969.7158.

Huang, X., and B. W. Reinisch (1982), Automatic calculation of electron density profiles from digital ionograms: 2. True height inversion of topside ionograms with the profile-fitting method, *Radio Sci.*, *17*(4), 837–844, doi:10.1029/RS017i004p00837.

Huang, X., B. W. Reinisch, D. Bilitza, and R. F. Benson (2002), Electron density profiles of the topside ionosphere, *Ann. Geophys.*, *45*(1), 125–130.

Jackson, J. E. (1969), The reduction of topside ionograms to electron-density profiles, *Proc. IEEE*, *57*, 960–976, doi:10.1109/PROC.1969.7140.

Jackson, J. E. (1986), Alouette-ISIS program summary, *NSSDC Rep., 86-09*, Natl. Space Sci. Data Cent., Greenbelt, Md.

Jackson, J. E. (1988), *Results from Alouette 1, Explorer 20, Alouette 2 and Explorer 31, NSSDC Rep., 88-10*, Natl. Space Sci. Data Cent., Greenbelt, Md.

Jackson, J. E., and E. S. Warren (1969), Objectives, history, and principal achievements of the topside sounder and ISIS programs, *Proc. IEEE*, *57*(6), 861–865, doi:10.1109/PROC.1969.7130.

Reinisch, B. W., and X. Huang (1982), Automatic calculation of electron density profiles from digital ionograms: 1. Automatic O and X trace identification for topside ionograms, *Radio Sci.*, *17*(2), 421–434, doi:10.1029/RS017i002p00421.

Reinisch, B. W., and X. Huang (1983), Automatic calculation of electron density profiles from digital ionograms: 3. Processing of bottomside ionograms, *Radio Sci.*, *18*, 477–492, doi:10.1029/RS018i003p00477.

Reinisch, B. W., P. Nsumei, X. Huang, and D. K. Bilitza (2007), Modeling the F2 topside and plasmasphere for IRI using IMAGE/RPI, and ISIS data, *Adv. Space Res.*, *39*, 731–738, doi:10.1016/j.asr.2006.05.032.

R. F. Benson, NASA Goddard Space Flight Center, Code 673, Greenbelt, MD 20771, USA. (robert.f.benson@nasa.gov)

D. Bilitza, School of Physics, Astronomy, and Computational Sciences, George Mason University, Fairfax, VA 22030, USA.

X. Huang, Center for Atmospheric Research, University of Massachusetts Lowell, Lowell, MA 01854, USA.

V. Truhlik, Institute of Atmospheric Physics, Academy of Sciences of the Czech Republic, 14131 Prague, Czech Republic.

Y. Wang, Goddard Planetary Heliophysics Institute, University of Maryland Baltimore County, NASA Goddard Space Flight Center, Code 674, Greenbelt, MD 20771, USA.